Theoretical Characterization of Proton-Induced Spectral Shifts in Schiff Base Porphyrins

James D. Petke* and Gerald M. Maggiora*

Contribution from the Departments of Chemistry and Biochemistry, University of Kansas, Lawrence, Kansas 66045. *Received August 8, 1983*

Abstract: The roles that substituents and protonation play in the electronic structure and spectrum of the Schiff base of magnesium 4-vinyl-8-formylporphine (MgPSB) have been investigated by ab initio self-consistent-field molecular orbital and configuration interaction calculations, using a floating spherical Gaussian orbital basis. The red shift of the visible band of the parent magnesium porphine (MgP) due to the presence of electron-withdrawing vinyl and Schiff base substituents is shown to arise from a small but significant destabilization of the highest occupied MgP π-orbital brought about by its conjugative interaction with the π-orbitals of the substituents. Changes in the ground-state electron density, however, result from larger perturbations of lower lying MgP orbitals. Protonation of the Schiff base leads to a dramatic differential stabilization of the high-lying π^*-orbital of the Schiff base moiety, giving rise to new orbital interactions with low-lying MgP π^*-orbitals that significantly alter the π^*-orbital structure of MgPSB. These changes, which affect only the excited states, are shown to be largely responsible for the additional proton-induced red shift ($\sim$1000 cm^{-1}) of the visible band and the unique doublet structure of the Soret band observed experimentally.

The effect of substituents on the electronic structures and spectra of porphyrins and metalloporphyrins is a topic that historically has been the focus of considerable study.[1-5] Recently, there has been renewed interest in this subject, particularly with respect to the formyl- and vinyl-substituted iron porphyrins which occur naturally as prosthetic groups in heme proteins and cytochromes. It has been proposed that biologically significant changes in porphyrin electronic structural properties may be effected through interaction of the substituents with the surrounding polypeptide chains.[6-8] These conjectures have led in turn to the synthesis and experimental characterization of a number of new substituted model porphyrins.[9-11] One of these, a Ni(II) porphyrin Schiff base (NiPSB)[12] prepared by Ward et al.,[11] is unusual in that it exhibits large changes in its absorption spectrum upon protonation, including a $\sim$1200-cm^{-1} red shift of the visible band and a dramatic change in the Soret region from a single relatively sharp, intense peak to two peaks of lower intensity, a feature uncharacteristic of the usual metalloporphyrin Soret band. The red shift of the visible band is reminiscent of the shifts observed, relative to monomeric chlorophyll, in the visible bands of P700 and P680, the photoactive pigments found in reaction centers of photosystems I and II, respectively, of green plants.[13] Hence, it has recently been proposed that a Schiff base chlorophyll may be a suitable candidate for P700 or P680.[14]

The present paper reports the results of an ab initio quantum mechanical study of the Schiff base of magnesium 4-vinyl-8-formylporphine (MgPSB) shown in Figure 1. Ab initio self-consistent-field molecular orbital (SCF MO) and configuration interaction (CI) calculations are employed to obtain ground- and excited-state wave functions, transition energies, and oscillator strengths for both protonated and nonprotonated forms of MgPSB. In addition, a detailed theoretical analysis, based on simple qualitative concepts, is presented to elucidate the effects of the substituents and of protonation on the electronic structure and spectrum of this molecule.

Calculations

The calculations reported here are similar to those previously employed in studies of porphyrins,[15] chlorophylls,[16] and other conjugated, macrocyclic molecules.[17] The computations include ab initio SCF MO studies on the ground state of each molecule using a basis set of floating spherical Gaussian orbitals (FSGO),[18] followed by calculation of ground- and excited-state wave functions using a multireference single and double excitation CI procedure. The details of these procedures may be found in previous publications.[15,16]

Due to the limited flexibility of the FSGO basis, the calculated transition energies, ΔE^{calcd}, obtained by this method are generally too large compared with experimental values. In previous studies of unsubstituted porphyrins[15] and chlorophylls[16] a linear equation (eq 1) giving reasonable estimated transition energies, ΔE^{estd}, from

$$\Delta E^{estd} = 0.610\Delta E^{calcd} - 441.0 \text{ (in cm}^{-1}\text{)} \quad (1)$$

the ΔE^{calcd}, was developed. This equation is used in the present work as well for comparisons with experimental data and with previous results on unsubstituted magnesium porphine (MgP).[15] Moreover, since the effect of protonation merely enhances the electron-withdrawing power of the SB substituent, it is not expected to affect the applicability of eq 1 in any substantial way.

For the molecular geometry of MgPSB, shown in Figure 1, the nuclear coordinates of the porphyrin macrocycle were chosen to be the same planar, 4-fold symmetric arrangement used for unsubstituted MgP.[15] This is reasonable in view of the crystal coordinates of a 4,8-diformyl free-base porphyrin,[9] which show

(1) Fischer, H.; Orth, H. "Die Chemie des Pyrrols"; Akad. Verlagsgesellschaft: Leipzig, 1937; Vol. 2.
(2) Falk, J. E. "Porphyrins and Metalloporphyrins"; Elsevier: New York, 1964.
(3) Phillips, J. N. In "Comprehensive Biochemistry"; Florkin, M., Stotz, E. H., Eds.; Elsevier: New York, 1963; Vol. 9.
(4) Caughey, W. S.; Fujimoto, Y.; Johnson, B. P. *Biochemistry* **1966**, *5*,, 3830-3843.
(5) Gouterman, M. *J. Chem. Phys.* **1959**, *30*, 1139-1161.
(6) Babcock, G. T.; Salmeen, I. *Biochemistry* **1979**, *18*, 2493-2498.
(7) Babcock, G. T.; Chang, C. K. *FEBS Lett.* **1979**, *97*, 358-362.
(8) Warshel, A.; Weiss, R. M. *J. Am. Chem. Soc.* **1981**, *103*, 446-451.
(9) Chang, C. K.; Hatada, M. H.; Tulinsky, A. *J. Chem. Soc., Perkin Trans. 2* **1983**, 371-378.
(10) Clezy, P. S.; Fookes, C. J. R. *Aust. J. Chem.* **1980**, *33*, 575-583.
(11) Ward, B.; Callahan, P. M.; Young, R.; Babcock, G. T.; Chang, C. K. *J. Am. Chem. Soc.* **1983**, *105*, 634-636.
(12) The molecule in question is the Schiff's base of nickel(II) 2,6-di-*n*-pentyl-4-vinyl-8-formyl-1,3,5,7-tetramethylporphine, where the substitutions correspond to the numbering system shown in Figure 1.
(13) Sauer, K. *Annu. Rev. Phys. Chem.* **1979**, 30, 155-178.
(14) Maggiora, L. L.; Maggiora, G. M. *Photochem. Photobiol.*, in press, and references cited therein.
(15) Petke, J. D.; Maggiora, G. M.; Shipman, L. L.; Christoffersen, R. E. *J. Mol. Spectrosc.* **1978**, *71*, 64-84.
(16) Petke, J. D.; Maggiora, G. M.; Shipman, L. L.; Christoffersen, R. E. *Photochem. Photobiol.* **1979**, *30*, 203-223; **1980**, *32*, 399-414.
(17) (a) Nitzsche, L. E.; Chabalowski, C.; Christoffersen, R. E. *J. Am. Chem. Soc.* **1976**, *98*, 4794-4801. (b) Murk, D.; Nitzsche, L. E.; Christoffersen, R. E. *Ibid.* **1978**, *100*, 1371-1378. (c) Petke, J. D.; Butler, P.; Maggiora, G. M. *Int. J. Quantum Chem.*, in press.
(18) Christoffersen, R. E.; Spangler, D.; Hall, G. G.; Maggiora, G. M. *J. Am. Chem. Soc.* **1973**, *95*, 8526-8536.

0002-7863/84/1506-3129$01.50/0

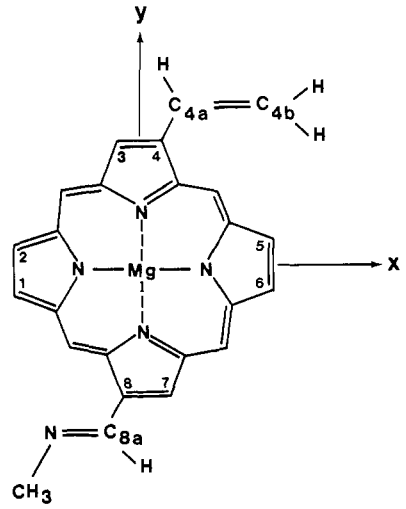

Figure 1. Molecular geometry of MgPSB.

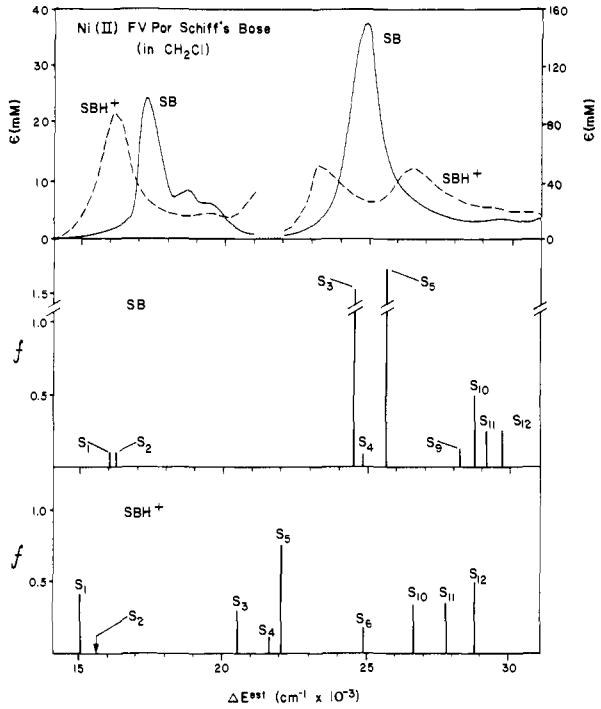

Figure 2. Comparison of the experimental spectrum (adapted from ref 11) of NiPSB and NiPSBH$^+$ (top) with the calculated spectra of MgPSB(30) (middle) and MgPSBH$^+$(30) (bottom). The calculated transition energies are estimates based on eq. 1; f represents the computed oscillator strength.

a high degree of planarity of the porphyrin skeleton. The vinyl coordinates and orientation were taken from crystal data on ethyl chlorophyllide *a*;[19] the group is positioned relative to the macrocyclic plane by a 30° rotation about the C_4–C_{4a} axis. The Schiff base coordinates were taken from a microwave spectrum of *N*-methylmethylenimine.[20] Two orientations of this substituent were studied: a 30° rotation of the substituent from the macrocyclic plane about the C_8–C_{8a} axis, MgPSB(30), and a 90° orientation, MgPSB(90), to determine the effects of macrocycle-substituent conjugation on molecular properties. Both substituents were rotated such that they lie on the same side of the macrocyclic plane and on the side opposite the magnesium ion.[15] Since the interaction of the substituent groups with the porphyrin macrocycle is primarily conjugative (vide infra) and since the two groups are well separated from each other, the side of macrocyclic plane on which they each lie is not expected to affect the results of the calculations significantly.

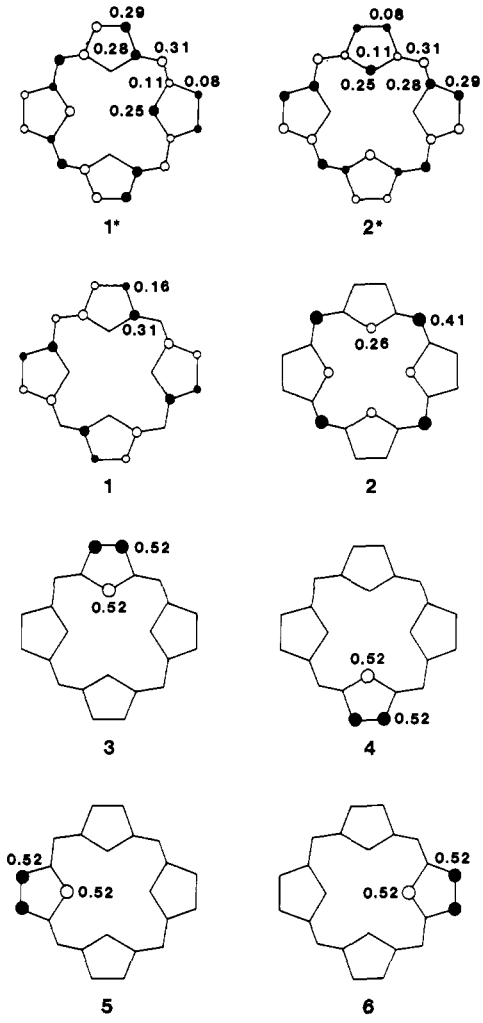

Figure 3. Spatial features of the six highest occupied π-orbitals, 1–6, and two lowest unoccupied π^*-orbitals, 1* and 2*, or MgP, given in terms of the contributions of positive (filled circles) and negative (open circles) p_π basis functions. Orbitals 3–6 shown are linear combinations of canonical SCF orbitals 3–6 of MgP, which are approximately degenerate. The linear combinations are chosen to produce orbitals with spatial characteristics similar to those of the corresponding orbitals of MgPSB and MgPSBH$^+$.

Results and Discussion

Non-Protonated Schiff Base. The experimental spectrum of NiPSB reported by Ward et al.[11] is reproduced in Figure 2 on a wavenumber scale. It is a typical metalloporphyrin spectrum, with a weak visible band at 17 330 cm^{-1} (577 nm) and an intense band in the Soret region at 24 750 cm^{-1} (404 nm). The visible band is red-shifted by approximately 800 cm^{-1} relative to the visible band of nickel octaethylporphine[21] (both spectra taken in CH_2Cl_2). This red shift is typical of those induced by electron-withdrawing substituents.[2-4] The Soret band of NiPSB is also red-shifted by 800 cm^{-1} relative to nickel octaethylporphine.[21]

The calculated spectrum of MgPSB(30) is also shown in Figure 2 and is very similar to that of MgP.[15] The visible and Soret bands of MgP are each composed of a pair of degenerate $\pi \rightarrow \pi^*$ transitions: in MgPSB(30) the degeneracy in the visible band is not appreciably altered, while the transitions in the Soret band are split, but apparently not enough to produce a split Soret band profile. The excited-state compositions and computed oscillator

(19) Chow, H.-C.; Serlin, R.; Strouse, C. E. *J. Am. Chem. Soc.* **1975**, *97*, 7230–7237.
(20) Sastry, K. V. L. N.; Curl, R. F. *J. Chem. Phys.* **1964**, *41*, 77–80.
(21) Edwards, L.; Dolphin, D. H.; Gouterman, M. *J. Mol. Spectrosc.* **1970**, *35*, 90–109.

Table I. Estimated Transition Energies, ΔE^{estd}, Computed Oscillator Strengths, f, and Compositions of the Electronic Singlet States of MgPSB(30) and $MgPSBH^+(30)$

	MgPSB(30)			MgPSBH$^+$(30)			
state	ΔE^{estd}, cm^{-1}	comp[a]	f	state	ΔE^{estd}, cm^{-1}	comp[a]	f
S_0	0.0	0.95 (SCF)		S_0	0.0	0.95 (SCF)	
S_1	16007	−0.59 (2 → 1*)	0.091	S_1	15036	0.83 (1 → 1*)	0.42
		0.74 (1 → 2*)				0.40 (2 → 2*)	
S_2	16164	0.74 (1 → 1*)	0.089	S_2	15624	0.71 (2 → 1*)	0.002
		−0.59 (2 → 2*)				−0.60 (1 → 2*)	
S_3	24516	0.61 (2 → 1*)	1.61	S_3	20530	0.51 (3 → 1*)	0.28
		0.52 (1 → 2*)				0.45 (2 → 2*)	
		0.27 (3 → 2*)				−0.50 (1 → 3*)	
						−0.30 (1^2 → 1^{*2})	
S_4	24793	0.74 (1 → 3*)	0.059	S_4	21653	−0.68 (3 → 1*)	0.097
		0.50 (1^2 → $\bar{1}$*,2*)				0.24 (2 → 2*)	
						−0.47 (1 → 3*)	
						−0.24 ($\bar{3}$,1 → 1^{*2})	
S_5	25612	0.54 (1 → 1*)	1.97	S_5	22014	0.49 (2 → 1*)	0.78
		0.66 (2 → 2*)				0.58 (1 → 2*)	
		−0.20 (3 → 2*)				0.44 (2 → 3*)	
S_6	26784	0.46 (3 → 1*)	5×10^{-4}	S_6	24880	−0.29 (1 → 1*)	0.17
		−0.56 (3 → 2*)				0.39 (2 → 2*)	
		−0.25 (4 → 2*)				0.22 (1 → 3*)	
						−0.32 (1 → 4*)	
						0.30 (1^2 → 1^{*2})	
						0.33 (2,$\bar{1}$ → $\bar{1}$*,2*)	
S_7	27259	−0.42 (3 → 1*)	0.002	S_7	25980	0.46 (4 → 1*)	0.084
		−0.23 (6 → 1*)				0.35 (5 → 1*)	
		0.51 (2 → 3*)				−0.57 (3 → 2*)	
		−0.25 (2,$\bar{1}$ → $\bar{1}$*,2*)					
		0.30 (2,$\bar{1}$ → 1*,$\bar{2}$*)					
S_8	27742	−0.53 (3 → 1*)	0.019	S_8	26033	−0.59 (5 → 1*)	0.008
		−0.26 (6 → 1*)				−0.56 (3 → 2*)	
		−0.26 (3 → 2*)				0.23 (5 → 2*)	
		−0.39 (2 → 3*)					
		0.23 (2,$\bar{1}$ → $\bar{1}$*,2*)					
		−0.28 (2,$\bar{1}$ → 1*,$\bar{2}$*)					
S_9	28296	0.47 (6 → 1*)	0.15	S_9	26407	−0.64 (4 → 1*)	0.042
		0.24 (7 → 1*)				0.31 (5 → 1*)	
		0.46 (3 → 2*)				−0.28 (3 → 2*)	
		0.28 (6 → 2*)				−0.22 (4 → 2*)	
						−0.24 (2 → 3*)	
						−0.21 ($\bar{4}$,1 → $\bar{1}$*,2*)	
S_{10}	28707	0.63 (4 → 1*)	0.43	S_{10}	26717	0.23 (4 → 1*)	0.35
		0.40 (7 → 1*)				−0.20 (5 → 1*)	
		−0.35 (4 → 2*)				0.43 (6 → 1*)	
						−0.38 (2 → 3*)	
						−0.28 (1^2 → $\bar{1}$*,2*)	
						−0.27 (2,$\bar{1}$ → 1^{*2})	
S_{11}	29123	0.31 (4 → 1*)	0.21	S_{11}	27749	0.51 (4 → 2*)	0.37
		−0.22 (6 → 1*)				−0.29 (1 → 3*)	
		0.65 (4 → 2*)				−0.25 (2 → 3*)	
		−0.20 (6 → 2*)				−0.32 (1 → 4*)	
		−0.20 (1^2 → 2^{*2})				0.20 (1^2 → $\bar{1}$*,2*)	
						−0.25 (2,$\bar{1}$ → 1^{*2})	
S_{12}	29684	0.50 (6 → 2*)	0.23	S_{12}	28762	0.26 (2 → 2*)	0.52
		−0.49 (1^2 → 1^{*2})				0.48 (4 → 2*)	
		−0.27 (7 → 1*)				0.33 (1 → 3*)	
		−0.24 (1^2 → 2^{*2})				−0.39 (1^2 → 1^{*2})	
		−0.30 (8 → 1*)				0.22 (2,$\bar{1}$ → $\bar{1}$*,2*)	

[a] Configurations with coefficients of magnitude >0.20 in the CI expansion of each state are listed and represented as orbital excitations with respect to the ground-state SCF single determinantal configuration. The occupied SCF orbitals are numbered in descending order (1 = the highest occupied orbital), and the unoccupied SCF orbitals are denoted by stars and numbered in ascending order (1* = the lowest unoccupied orbital). A bar denotes β spin.

strengths for S_1 and S_2 (visible band) and S_3 and S_5 (Soret band) of MgPSB(30) listed in Table I closely resemble those of the respective states reported for MgP.[15]

The computed spectrum of MgPSB(90) is qualitatively the same in every respect to that of MgPSB(30). However, the calculated visible band of MgPSB(90) is estimated to be red-shifted relative to MgP by only ~565 cm^{-1} as opposed to ~1100 cm^{-1} for MgPSB(30), implying that such spectral shifts are dependent on macrocycle-substituent conjugation.

To interpret the effect of the vinyl and Schiff base substituents on the electronic structure and spectrum of MgP, it is useful to consider the manner in which the MgP orbitals are perturbed by the substituents. In Figure 3 the general features of the six highest-lying orbitals (1–6) and two lowest-lying unoccupied orbitals (1*,2*) or MgP, obtained in a previous calculation,[15] are presented. Orbitals 3–6, which are approximately 4-fold degenerate in MgP, are represented not as the usual canonical SCF orbitals, but as linear combinations of SCF orbitals that possess

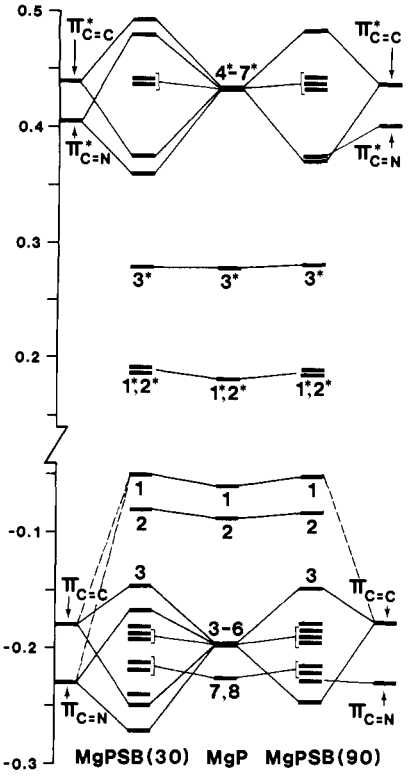

Figure 4. Molecular orbital energy level diagram (in atomic units) showing the orbitals of MgPSB and their correlations with MgP and substituent orbitals. MgP orbitals were taken from ref 15; C=C and C=N orbitals were obtained from SCF calculations on ethylene and *N*-methylmethylenimine, respectively. Solid lines connecting orbitals indicate the principal orbital correlations. Dotted lines indicate weaker but significant orbital correlations, which are discussed in the text.

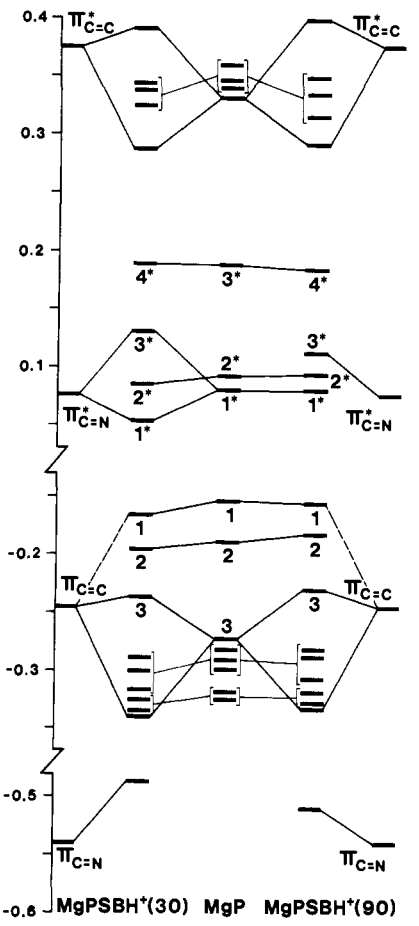

Figure 5. Molecular orbital energy level digram (in atomic units) showing the orbitals of $MgPSBH^+$ and their correlations with MgP and substituent orbitals. MgP, C=C, and C=N orbitals were obtained from SCF calculations on MgP, ethylene, and *N*-methylmethylenimine, respectively, in which an additional proton was placed at the same location relative to each molecule as in $MgPSBH^+(30)$. Solid lines connecting orbitals indicate the principal orbital correlations. Dotted lines indicate weaker but significant orbital correlations, which are discussed in text.

spatial characteristics consistent with the corresponding orbitals obtained for MgPSB(30).

Perturbations of the MgP orbitals by the interaction of substituent π- and π^*-orbitals are illustrated in Figure 4. The vinyl and Schiff base π^*-orbitals are seen to interact strongly only with the higher-lying π^*-orbitals of MgP, and therefore have no effect on the ground and low-lying excited states considered here. On the other hand, the substituent π-orbitals do interact strongly with orbitals 3 and 4 of MgP (only orbital 3 is perturbed in MgPSB-(90)), resulting in very specific conjugative electron-withdrawing effects within the π-electron system of the substituted pyrrole rings. The π-electron density within the unsubsttuted pyrrole rings is not significantly altered. It is important to realize, however, that while these perturbations are responsible for the principal changes in ground-state electron density, they are not responsible for the observed red shift of the visible band. As discussed below, the red shift is induced through a weaker interaction between the substituent π-orbitals and orbital 1 of MgP.

A fundamental concept in the description of metalloporphyrin spectra is the "four-orbital" model originated by Gouterman.[22] According to this approximation, S_1 and S_2 are each described by linear combinations of two configurations which arise from single excitations from occupied orbitals 1 and 2 to virtual orbitals 1* and 2*. Thus, it follows that changes in visible spectra must arise *primarily* through perturbations of these four orbitals. Figures 3 and 4 indicate that orbitals 1*, 2*, and 2 are largely unaffected by the substituent π-orbitals, the latter because there is negligible electron density at the points of substitution. However, antibonding interactions between orbital 1 and the substituent π-orbitals, although weaker than the perturbation of orbitals 3 and 4 described above, are primarily responsible for the red shift of the visible band. This may be seen by comparing the state compositions of S_1 and S_2 of MgPSB(30) shown in Table I with those of S_1 and S_2 of MgP.[15,23] While the compositions of S_1 and S_2 in both molecules are similar and typically "four orbital" in nature, in MgPSB(30) the additional conjugation of the substituent orbitals with orbital 1 results in excitations ($1 \rightarrow 1^*$) and ($1 \rightarrow 2^*$) being energetically more favorable than in MgP. Thus, the compositions of S_1 and S_2 of MgPSB(30) show a bias toward these excitations, which results in a lowering of the energies of S_1 and S_2 relative to the ground state, S_0. In MgPSB(90), only the vinyl group conjugates with orbital 1; consequently the calculated spectral red shift is less than in MgPSB(30). The red shift of the Soret band, however, appears to be due to the destabilization of *both* orbital 1 and orbital 3. This is evident from the data in Table I for Soret states S_3 and S_5 of MgPSB(30). These states contain appreciable contributions from excitations ($1 \rightarrow 1^*$), ($1 \rightarrow 2^*$), and ($3 \rightarrow 2^*$), all of which are energetically more favorable than they are in unsubstituted MgP.

The above analysis indicates that electron-withdrawing substituents, when conjugated to the porphyrin macrocycle at the β-carbon of the pyrrole ring, play a dual role in influencing electronic structure and spectra. Caughey et al.[4] have studied substituent effects on both visible spectra and nitrogen basicity in free-base porphyrins. That they failed to obtain a linear correlation between substituent-induced decreased in nitrogen basicity and spectral red shift is consistent with the fact that different orbital interactions are responsible for these two effects.

(22) (a) Gouterman, M. In "The Porphyrins"; Dolphin, D., Ed.; Academic Press: New York, 1977; Vol. 3. (b) *J. Mol. Spectrosc.* **1961**, *6*, 138–163.

(23) The state compositions of S_1 and S_2 of MgP given in ref 15 are $S_1 \sim -0.68(1 \rightarrow 2^*) + 0.61(2 \rightarrow 1^*)$ and $S_2 \sim -0.68(1 \rightarrow 1^*) + 0.61(2 \rightarrow 2^*)$. S_1 and S_2 are doubly degenerate in MgP.

The present analysis also suggests that larger spectral red shifts could in principle be obtained through substitution of more highly conjugated substituents at the β-carbons, which would interact more strongly with orbital 1. However, such substituents might be ineffective due to loss of conjugation from steric effects. Alternatively, an anionic substituent whose π- or π*-orbital is orbitally degenerate with orbital 1 of MgP could in principle induce large spectral changes through a strong conjugative interaction with this orbital.

Protonated Schiff Base. The spectrum of protonated NiPSB ($NiPSBH^+$) is shown in Figure 2, and it is clear that it differs significantly from that of NiPSB. As mentioned previously, protonation induces an $\sim$1200-cm^{-1} red shift of the visible band; in addition the Soret region is considerably different from that of NiPSB.

The calculated spectrum of protonated $MgPSBH^+(30)$ is also shown in Figure 2, and the computed electronic states are tabulated in Table I. It is clear from these data that the change in the Soret spectral region is not due simply to an increased splitting of the degenerate metalloporphyrin Soret band but to a complete change in the composition of the constituent electronic states. The proton-induced red shift of the visible band is estimated to be $\sim$1000 cm^{-1}. To ensure that the shift was not an artifact of the computational method, a larger (ca. 2000 configurations) CI calculation designed to obtain more highly converged wave functions specifically for S_0, S_1, and S_2 was carried out on MgPSB(30) and $MgPSBH^+(30)$. The energies and state compositions obtained differ insignificantly from those reported in Table I.

The effects of protonation may be understood by considering the orbital interaction diagram shown in Figure 5. In this figure the orbital energies of unsubstituted MgP and the vinyl and Schiff base substituents were obtained from SCF calculations on each isolated molecule with an additional proton placed so that its effect is equivalent to the proton in $MgPSBH^+(30)$. This accounts approximately for the effect of the proton nuclear charge alone on the noninteracting molecular orbitals. For $MgPSBH^+(30)$, Figure 5 shows that the vinyl orbitals interact with MgP orbitals in much the same manner as in the nonprotonated case. The Schiff base π-orbital is now much lower in energy due to the close proximity of the proton and does not perturb any of the higher lying MgP π-orbitals; it appears as an isolated "C=N" π-orbital among the orbitals of $MgPSBH^+(30)$. This explains why the ^1H NMR and resonance Raman spectra of $NiPSBH^+$ reported by Ward et al.[11] showed that protonation effects were localized at the Schiff base and did not perturb the porphyrin macrocycle.

The principal perturbation by a substituent orbital is clearly that produced by the energetically favorable interaction of the Schiff base π*-orbital with the 1* orbital of MgP, producing a set of three low-lying nondegenerate π*-orbitals in $MgPSBH^+(30)$, as opposed to a degenerate pair of π*-orbitals in MgPSB(30) and MgP. Thus, we have the unusual situation in which protonation of the ground state of MgPSB(30) results chiefly in changes in the nature and location of the low-lying excited states. The red shift of the visible band may be seen as being a consequence of the differential stabilization of S_1 relative to S_0 in $MgPSBH^+(30)$ due to the lower orbital energy of the 1* orbital, which causes the energetically favorable $1 \rightarrow 1^*$ excitation to become the dominant configuration in the CI composition of S_1 (see Table I). Additionally, the $S_1 \leftarrow S_0$ oscillator strength is seen to be larger than in MgPSB(30).

Among the higher lying electronic states given in Table I, it is evident that because of the new virtual orbital space, there are a number of states of moderately high oscillator strength that do not correlate with the higher lying states of MgPSB but that produce a calculated spectrum in the Soret region which is qualitatively consistent with that of $NiPSBH^+$, as shown in Figure 2.

Finally, it is also interesting to point out that the spectral effects of Schiff base protonation may be "switched off" if the Schiff base is not in conjugation with the macrocycle. This may be seen in Figure 5 for $MgPSBH^+(90)$, where these is no interaction between the Schiff base π*-orbital and the MgP 1*- and 2*-orbitals. Thus, in $MgPSBH^+(90)$ orbitals 1* and 2* are the same as in MgPSB(90), orbital 3* is an isolated "C=N" π*-orbital, and there is no significant change in the spectrum of MgPSB(90) upon protonation.

Acknowledgment. This work was supported by the Division of Chemical Sciences, Office of Basic Energy Sciences, U.S. Department of Energy. The authors thank Professor G. T. Babcock for providing a copy of his paper on protonated Schiff base porphyrins prior to publication.

Registry No. MgPSB, 89656-92-8; $MgPSBH^+$, 89675-82-1.

Vibrational Frequency Shifts in Hydrogen-Bonded Systems: The Hydrogen Fluoride Dimer and Trimer

Jeffrey F. Gaw, Yukio Yamaguchi, Mark A. Vincent, and Henry F. Schaefer III*

Contribution from the Department of Chemistry and Lawrence Berkeley Laboratory, University of California, Berkeley, California 94720. *Received November 10, 1983*

Abstract: Ab initio molecular electronic structure theory has been used to predict the structures and harmonic vibrational frequencies of $(HF)_2$ and $(HF)_3$. Standard Huzinaga-Dunning double-ζ (DZ) and double-ζ plus polarization (DZ+P) basis sets have been used in conjunction with self-consistent-field (SCF) and configuration-interaction (CI) methods. As many as 29 161 configurations were included variationally, with analytic CI gradient methods used to precisely locate stationary point geometries. The DZ SCF, DZ+P SCF, and DZ+P CI methods all give qualitative agreement with recent high-resolution spectroscopic measurements of the H-F dimer vibrational frequency shifts. Trimer equilibrium and transition-state structures and vibrational frequencies have similarly been predicted at the DZ SCF and DZ+P SCF levels of theory.

One of the most important new developments in molecular spectroscopy is the potential for the determination of the high-resolution vibrational spectra of hydrogen-bonded systems. An excellent example of these advances is given by Pine and Lafferty's recent study[1] of rotational structure and vibrational predissociation in the HF stretching bands of the HF dimer. Pine and Lafferty's high-resolution infrared study appears to establish the "free" hydrogen H-F stretch ν_1 at 3929 cm^{-1} and the "bonded" hydrogen H-F fundamental ν_2 at 3868 cm^{-1}. Compared to the HF monomer fundamental[2] at 3961 cm^{-1}, these new experiments indicate dimer

(1) A. S. Pine and W. J. Lafferty, *J. Chem. Phys.*, **78**, 2154 (1983).

(2) G. Guelachvili, *Opt. Commun.*, **19**, 150 (1976).

0002-7863/84/1506-3133$01.50/0